Taper-Like Longitudinal Variations in Etched SMS Fibers Modal Evolution and Spectral Response for Optical Sensing

Natalia Lara-Davila and Jorge Montoya-Cardona
Department of Electronics and Telecommunications, Institución Universitaria ITM, Medellín 050026, Colombia

INTRODUCTION

The spectral response of etched SMS fiber sensors arises from multimode interference in the MMF section. However, most analyses assume longitudinally uniform etched geometries, where modal power remains nearly invariant along propagation. Here, we compare a uniform E-SMS structure with a taper-like etched SMS configuration to examine how axial diameter variations modify modal evolution, external-field interaction, and spectral response.

COMPUTATIONAL FRAMEWORK

The two SMS configurations were numerically modeled in FIMMWAVE using SMF-28 and a coreless MMF FGLA125. Three complementary analyses were performed: longitudinal normalized modal power, external interaction factor, and spectral response.

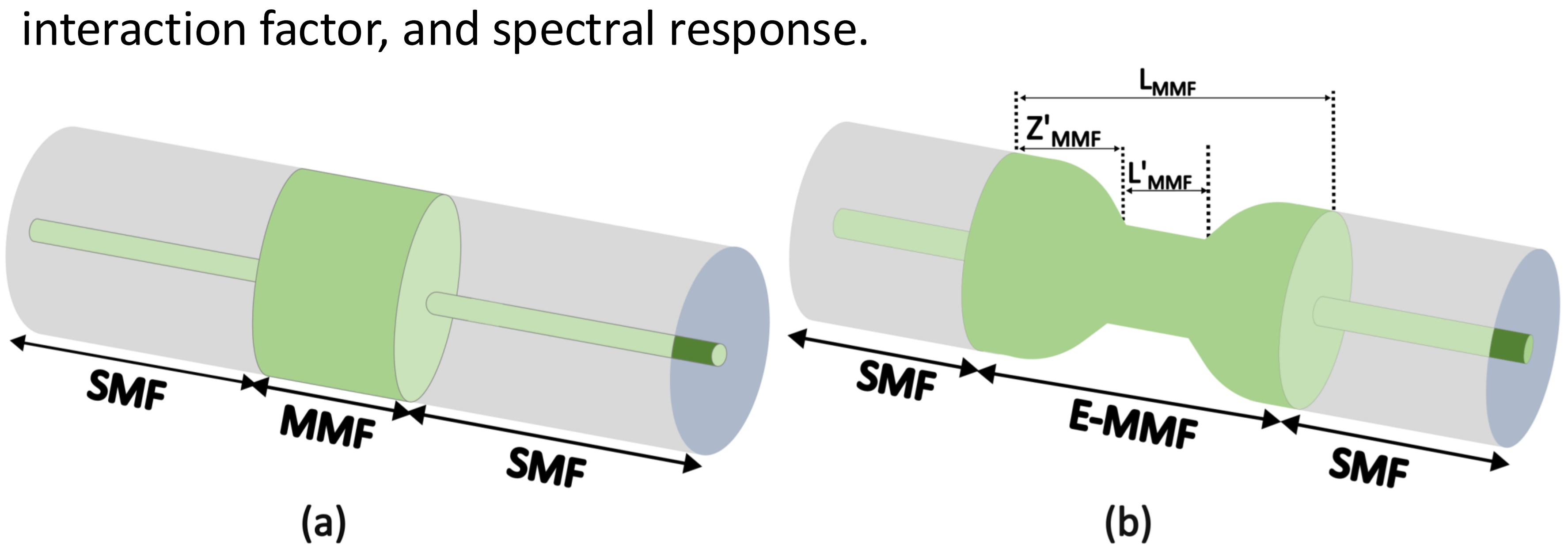

Figure 1. Uniform (a) and taper-like (b) etched SMS structures used in this work.

The local modal power was obtained through the normalized overlap integral,

$$P_m(z) = \left| \frac{\iint_A E_{p,t}(x,y;z) \times H^*_{m,t}(x,y) \cdot \hat{z}\, dA}{\iint_A E_{m,t}(x,y) \times H^*_{m,t}(x,y) \cdot \hat{z}\, dA} \right|^2$$

and the normalized modal power was defined as $\tilde{P}_m(z) = P_m(z)/\sum_{n=1}^{M} P_n(z)$ where (m) denotes the selected mode and (M) the total number of included modes. In the uniform E-SMS structure, $P_m(z)$ remains nearly invariant along (z), whereas in the taper-like configuration it evolves with the local diameter variation.

The external interaction factor was computed from the electric-field energy in the surrounding region,

$$\Gamma(z) = \frac{\iint_{A_{ext}(z)} |E(x,y;z)|^2\, dA}{\iint_A |E(x,y;z)|^2\, dA}$$

where $A_{ext}(z)$ is defined from the local etched geometry.

Finally, the spectral response was evaluated from the normalized transmitted power at the output SMF as a function of wavelength,

$$T(\lambda) = \frac{P_{out}(\lambda)}{P_{in}(\lambda)}$$

Table 1. Geometrical parameters of the analyzed SMS configurations.

Parameter	Uniform E-SMS	Taper-like E-SMS
SMF length	$10\ mm$	$10\ mm$
MMF length (L_{MMF})	$15\ mm$	$15\ mm$
Initial MMF diameter	$125\ \mu m$	$125\ \mu m$
Minimum etched diameter	$40\ \mu m$	$40\ \mu m$
Taper-down length (Z'_{MMF})	–	$2.5\ mm$
Waist length (L'_{MMF})	–	$10\ mm$
Taper-up length (Z'_{MMF})	–	$2.5\ mm$

RESULTS & DISCUSSION

In the uniform E-SMS structure, $\tilde{P}_m(z)$ remains nearly invariant along propagation, providing the reference case for the taper-like geometry.

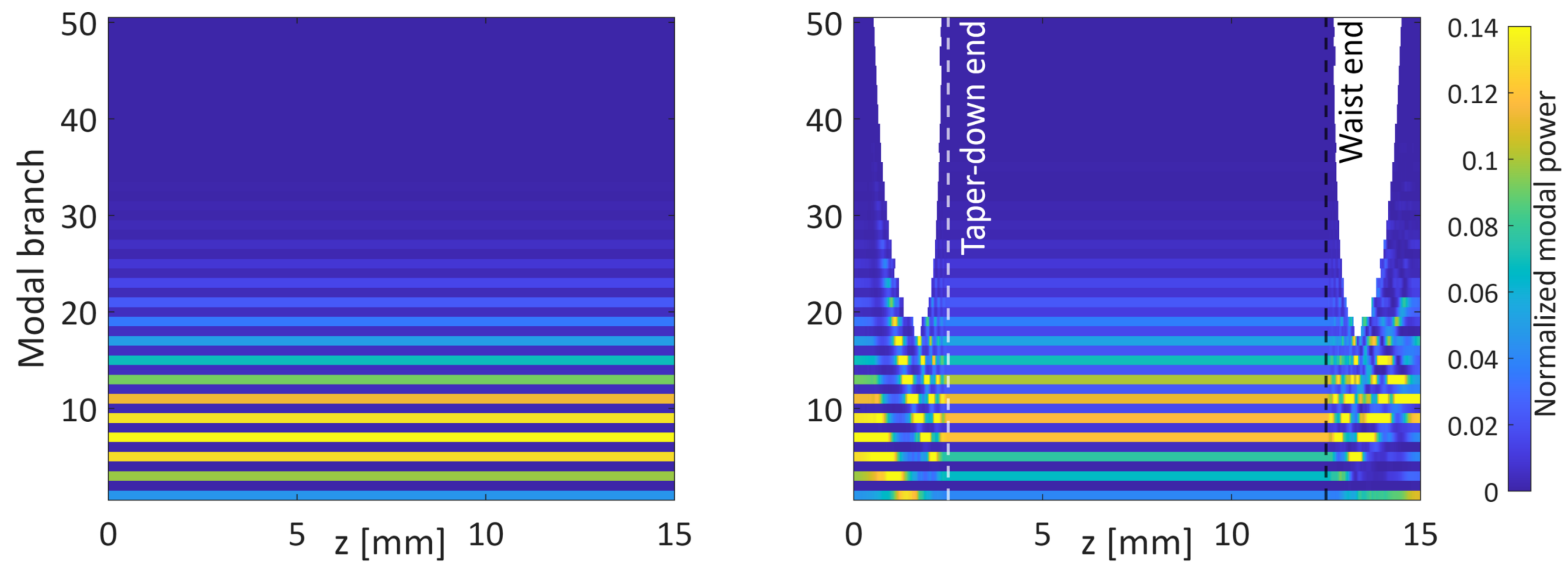

Figure 2. Longitudinal normalized modal power $\tilde{P}_m(z)$ for the uniform E-SMS (left) and taper-like E-SMS (right) structures at 40 μm minimum diameter.

The external interaction factor $\Gamma(z)$ quantifies the percentage of optical-field energy in the surrounding region along the device. In the taper-like E-SMS structure, $\Gamma(z)$ varies with the local diameter, unlike the more stable behavior of the uniform case.

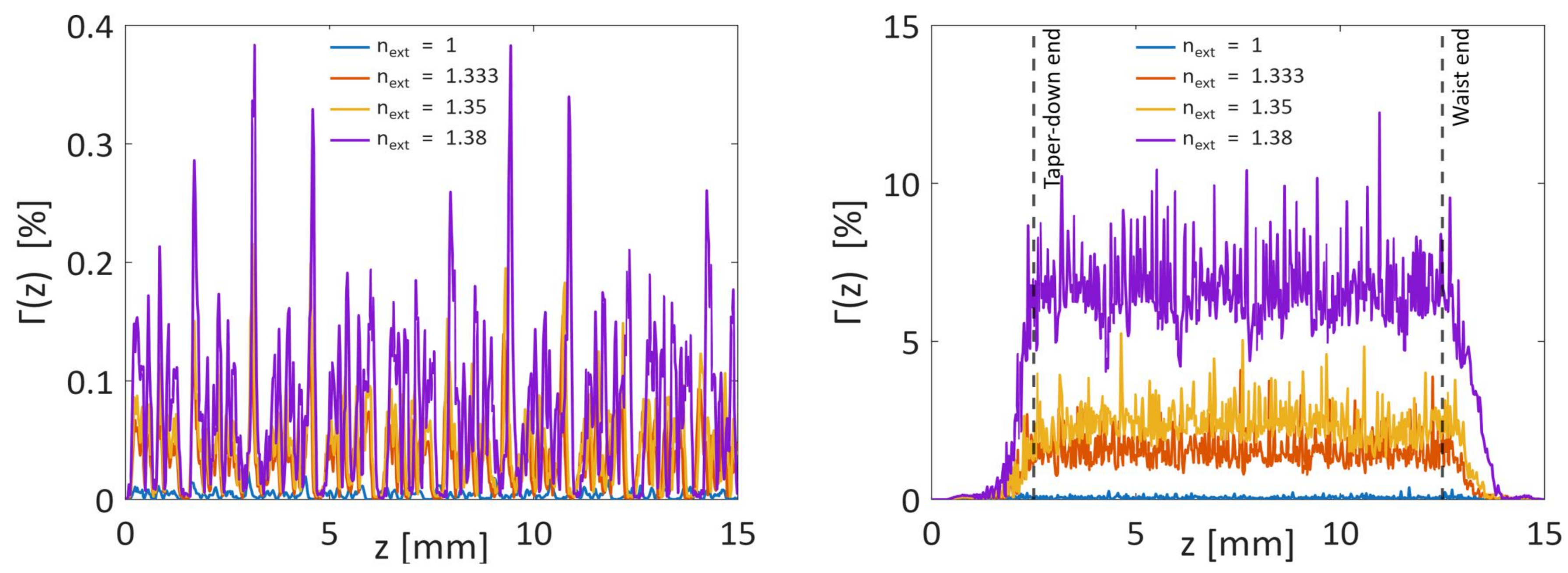

Figure 3. External interaction factor $\Gamma(z)$ for the uniform E-SMS (left) and taper-like E-SMS (right) structures under different external refractive indices (n_{ext}).

The refractometric response was quantified from the resonance wavelength shift λ_{res} as a function of the external refractive index. The sensitivity was estimated from $(S = d\lambda_{res}/dn_{ext})$ for the uniform and taper-like E-SMS structures.

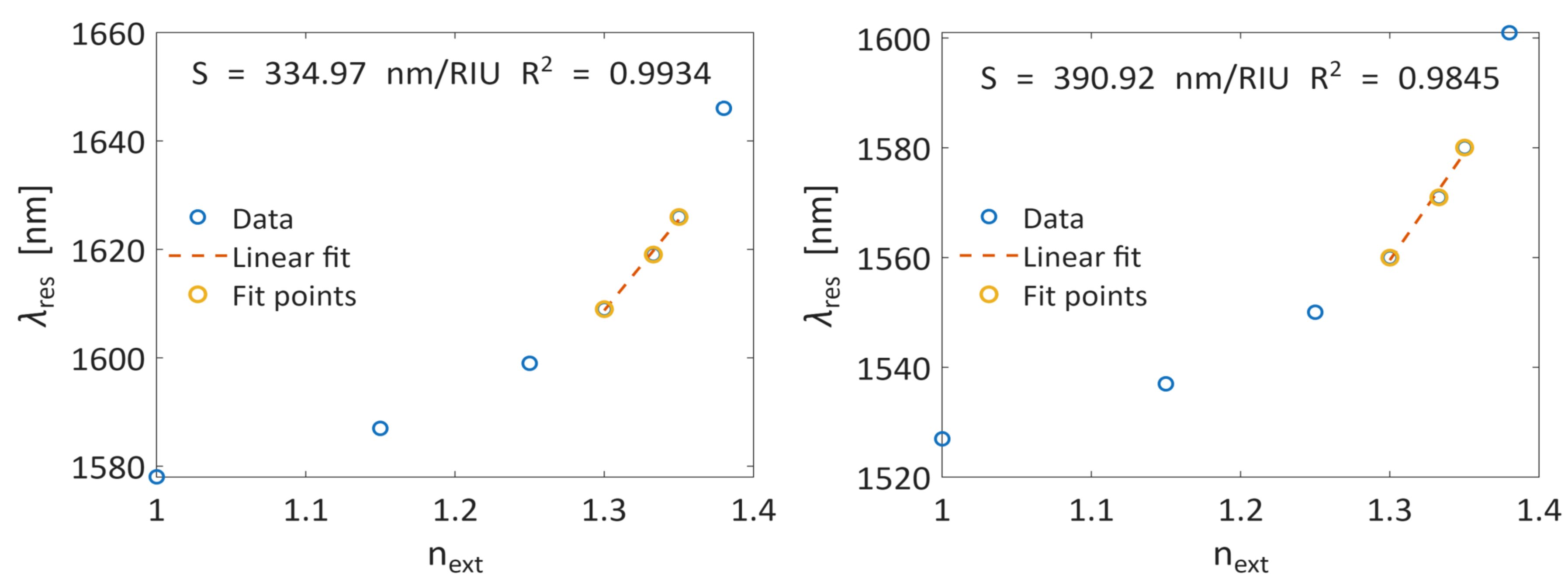

Figure 4. Resonance wavelength λ_{res} versus external refractive index for the uniform (left) and taper-like (right) E-SMS structures.

CONCLUSION

The taper-like E-SMS configuration induces a clear longitudinal modal redistribution and significantly increases the external-field interaction compared with the uniform structure. However, the spectral sensitivity exhibits only a moderate improvement, indicating that enhanced field exposure alone does not determine the resonance shift, which also depends on the overall modal interference process.

REFERENCES

[1] Lara Davila, N.; Montoya Cardona, J.A. Proceedings of the 1st IOCO, 25–27, MDPI: Basel, Switzerland.
[2] Lara-Davila, N.C.; Montoya-Cardona, J.A.; Gonzalez-Valencia, E. Eng. Proc. 2025, 118, 32.